JACS
JOURNAL OF THE AMERICAN CHEMICAL SOCIETY

Article

pubs.acs.org/JACS

Generation of Singlet Oxygen by the Glyoxal–Peroxynitrite System[‖]

Júlio Massari,[†] Rita Tokikawa,[‡] Danilo B. Medinas,[‡] José P. F. Angeli,[‡] Paolo Di Mascio,[‡] Nilson A. Assunção,[§] and Etelvino J. H. Bechara*[,‡,§]

[†]Departamento de Química Fundamental and [‡]Departamento de Bioquímica, Instituto de Química, Universidade de São Paulo, São Paulo, SP, Brazil

[§]Instituto de Ciências Ambientais, Químicas e Farmacêuticas, Universidade Federal de São Paulo, Diadema, SP, Brazil

ABSTRACT: Diacetyl, methylglyoxal, and glyoxal are α-dicarbonyl catabolites prone to nucleophilic additions of amino groups of proteins and nucleobases, thereby triggering adverse biological responses. Because of their electrophilicity, in aqueous medium, they exist in a phosphate-catalyzed dynamic equilibrium with their hydrate forms. Diacetyl and methylglyoxal can be attacked by peroxynitrite ($k_2 \approx 1.0 \times 10^4$ M^{-1} s^{-1} and $k_2 \approx 1.0 \times 10^5$ M^{-1} s^{-1}, respectively), a potent biological nucleophile and oxidant, yielding the acetyl radical from the homolysis of peroxynitrosocarbonyl adducts, and acetate or formate ions, respectively. We report here that glyoxal also reacts with peroxynitrite, yielding formate ion at rates at least 1 order of magnitude greater than does methylglyoxal. A triplet EPR signal (1:2:1; a_H = 0.78 mT) attributable to hydrated formyl radical was detected by direct flow experiments. In the presence of the spin trap 2-methyl-2-nitrosopropane, the EPR spectrum displays the di-*tert*-butyl nitroxide signal, another signal assignable to the spin trapping adduct with hydrogen radical ($a_N = a_H$ = 1.44 mT), probably formed from formyl radical decarbonylation, and a third EPR signal assignable to the formyl radical adduct of the spin trap (a_N = 0.71 mT and a_H = 0.14 mT). The novelty here is the detection of singlet oxygen ($^1\Delta_g$) monomol light emission at 1270 nm during the reaction, probably formed by subsequent dioxygen addition to formyl radical and a Russell reaction of nascent formylperoxyl radicals. Accordingly, the near-infrared emission increases upon raising the peroxynitrite concentration in D_2O buffer and is suppressed upon addition of O_2 ($^1\Delta_g$) quenchers (NaN_3, L-His, H_2O). Unequivocal evidence of O_2 ($^1\Delta_g$) generation was also obtained by chemical trapping of $^{18}O_2$ ($^1\Delta_g$) with anthracene-9,10-divinylsulfonate, using HPLC/MS/MS for detection of the corresponding 9,10-endoperoxide derivative. Our studies add insights into the molecular events underlying nitrosative, oxidative, and carbonyl stress in inflammatory processes and aging-associated maladies.

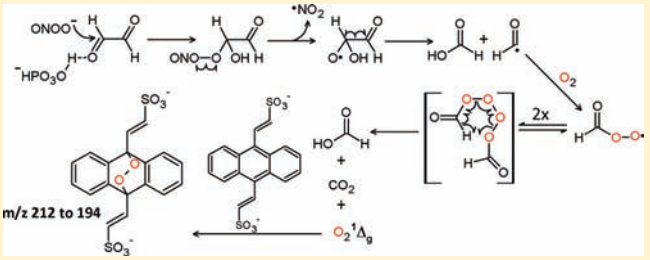

INTRODUCTION

Ethanedial (glyoxal) is a highly reactive dialdehyde present in food,[1,2] beverages,[3−5] cigarette smoke,[6] and urban air.[7−9] In biological samples, glyoxal has been found as an end product of the aerobic oxidation of carbohydrates, proteins, polyunsaturated fatty acids, and nucleic acids.[10−13] Like other α-dicarbonyl metabolites (e.g., methylglyoxal, 2,3-butanedione, 4,5-dioxopentanoic acid, and deoxygluxasones), glyoxal is reportedly implicated in Maillard reactions which may lead to a metabolic condition usually named "carbonyl stress".[13]

Methylglyoxal[14] and butanedione (diacetyl)[15] were recently shown to undergo nucleophilic attack by peroxynitrite at much faster rates ($k_2 \approx 1 \times 10^5$ M^{-1} s^{-1} and $k_2 \approx 1 \times 10^4$ M^{-1} s^{-1}, respectively, at pH 7.2, 25 °C)[14−16] than do monocarbonyls ($<10^3$ M^{-1} s^{-1}),[17,18] ultimately yielding formate and acetate, or acetate ions, respectively. Importantly, the rate constant of the reaction of peroxynitrite with methylglyoxal is roughly 3-fold greater than with HCO_3^-/CO_2,[19] which is noted as the main intracellular target of peroxynitrite in cells. In addition to acting as a powerful nucleophile, peroxynitrite is able to directly and indirectly promote one- and two-electron oxidations, nitrosation, and nitration of biomolecules. A broad set of peroxynitrite final products has been identified and adopted as biomarkers in human disorders such as Alzheimer's disease, rheumatoid arthritis, atherosclerosis, lung injury, amyotrophic lateral sclerosis, diabetes, cancer, and drug-dependent toxicity.[19−27]

Here, we report that nucleophilic addition of peroxynitrite to glyoxal in normally aerated phosphate buffer produces molecular oxygen in the singlet excited state ($^1\Delta_g$). Generation of singlet oxygen, O_2 ($^1\Delta_g$), was assessed through the direct spectroscopic detection of its monomol light emission at 1270 nm, as well as by the observation of D_2O enhancement of O_2 ($^1\Delta_g$) production and the quenching effect of sodium azide. In addition, the reaction mechanism was investigated by chemically trapping the O_2 ($^1\Delta_g$) produced in the reaction using the anthracene-9,10-divinylsulfonate anion (AVS). The chemical trapping method was coupled to the detection of the corresponding endoperoxide $AVSO_2$ by HPLC coupled to UV and mass spectrometry in tandem. In light of previous work by Uppu et al.[17] and Nakao et al.[18] on the reaction of

Received: June 3, 2011
Published: November 18, 2011

peroxynitrite with carbonyls, the glyoxal reaction is envisaged as initial peroxynitrite addition to yield a hypothetical nitrosoperoxy adduct, whose homolysis yields $^{\bullet}NO_2$ and a glyoxal-derived oxyl radical.

$$CHO{-}CHO + ONOO^{-} \rightarrow CHO{-}CH(O^{-})OONO \rightarrow CHO{-}CH(O^{-})O^{\bullet} + {}^{\bullet}NO_2$$

Subsequently, β-cleavage of the oxyl radical would generate formyl radical and formate ion, followed by reaction of formyl radical with molecular oxygen to yield a formylperoxyl radical.

$$CHO{-}CH(O^{-})O^{\bullet} \rightarrow {}^{\bullet}CHO + HCO_2^{-}$$

$$^{\bullet}CHO + O_2 \rightarrow CHO{-}OO^{\bullet}$$

Annihilation of alkylperoxyl radicals by the Russell reaction is long known to generate 3−14% O_2 ($^1\Delta_g$) and, at 3−4 orders of magnitude lower yield, triplet carbonyls.[28] Bearing a geminal hydrogen atom, the formylperoxyl radical is endowed with the potential of producing O_2 ($^1\Delta_g$) by the Russell reaction.[29−33]

$$2CHO{-}OO^{\bullet} \rightarrow [CHO{-}OOOO{-}CHO] \rightarrow CH_2O + CO_2 + O_2(^1\Delta_g)$$

MATERIALS AND METHODS

Chemicals and Reagents. All reagents were purchased, with a high grade of purity, from Sigma-Aldrich (St. Louis, MO), Merck (Darmstadt, Germany), and Fluka (Buchs, Switzerland). The $^{18}O_2$ gas cylinder (99% ^{18}O) was from Isotec-Sigma (St. Louis, MO). Peroxynitrite was synthesized from $NaNO_2$ (0.60 M) and H_2O_2 (0.70 M) in HCl (0.60 M) and NaOH (1.50 M) in a quench-flow reactor as described previously.[14,34] Excess H_2O_2 in the alkali peroxynitrite solution was eliminated with MnO_2; however, nitrite and nitrate ions derived from peroxynitrite decomposition usually remain as contaminant ions. Concentrations of H_2O_2 and peroxynitrite were determined spectrophotometrically at 240 (ε = 42 M^{-1} cm^{-1})[35] and 302 nm (ε = 1670 M^{-1} cm^{-1}),[34,36] respectively. The peroxynitrite concentrations obtained by this method ranged from 300 to 450 mM. Stock solutions of peroxynitrite were kept on ice in the dark. Sodium anthracene-9,10-divinylsulfonate, a O_2 ($^1\Delta_g$) chemical trap, was prepared and purified according to procedures described elsewhere.[37,38]All the solutions were prepared in Millipore Milli-Q purified water, and the buffers were pretreated with Chelex-100 to remove metal contaminants.

Stopped-Flow Kinetics. The rate of peroxynitrite decay was monitored with a stopped-flow spectrophotometer (Applied Photophysics model SX-18V) at 302 nm. The temperature was kept constant at 25.0 ± 0.2 °C, and the pH values of the reaction mixtures were determined by an experiment in Eppendorf tubes under the same conditions. The initial concentration of peroxynitrite was at 200 μM. Pseudo-first-order rates, k_{obs} (s^{-1}), were determined by linear fit from ln A vs time (0−30 ms), and the first linear fit observed was assumed as the k_{obs} (s^{-1}). The results of 9−12 measurements were averaged to obtain each rate constant. The apparent second-order rate constant ($k_{2,app}$) was calculated from slopes of the plots of k_{obs} vs the glyoxal concentration. The rate of peroxynitrite decay in the buffer solution, k_0, was subtracted from k_{obs} before plotting data against pH or phosphate buffer concentration. All the data were fitted using Origin 7 (Microcal Software, Inc.).

Continuous-Flow EPR Studies. The experiments were conducted at room temperature (25 ± 2 °C) in a Bruker EMX spectrometer equipped with a Bruker ER 4117 D-MTV dielectric mixing resonator with 9 mm of distance between the mixing cell and the resonator center. Briefly, the reactants were loaded in 20 mL plastic syringes mounted on a pump (Harvard Apparatus pump 22) and driven into the resonator at constant flow. Experimental conditions and equipment settings are described in the captions to the figures. The magnetic field was calibrated with the nitroxide 4-hydroxy-2,2,6,6-tetramethylpiperidine-*N*-oxyl (TEMPOL), whose g value is 2.0056. Computer simulations of spectra were performed by using the program WINSIM written by Duling.[39]

Singlet Oxygen Detection. Monomolecular photoemission of $O_2(^1\Delta_g)$ at 1270 nm was monitored by a photocounting equipment as described previously.[40,41] For this purpose, reaction mixtures of glyoxal (0−10 mM) and peroxynitrite (2.5 mM) were analyzed in the photon counter. The reaction was carried out in D_3PO_4 solution in D_2O, resulting in a pD between 7.1 and 7.5 by the addition of the alkali solution of peroxynitrite at 25 °C in the dark. All reactions were conducted in a quartz cuvette under continuous stirring at room temperature. The apparatus consists of a photomultiplier tube cooled to −80 °C with liquid nitrogen to reduce the dark current. The power was provided by a high voltage DC power supply, and the applied potential was set to −1.5 kV. The light emitted from the sample was processed with a diffraction grate capable of selecting wavelenghts in the infrared region. The phototube output was connected to the computer and the signal acquired digitally.

Chemical Trapping of Singlet Oxygen. The generation of O_2 ($^1\Delta_g$) during the reaction of glyoxal and peroxinitrite was monitored by chemical trapping with AVS. For this purpose, glyoxal (0−10 mM) and peroxynitrite (2.5 mM) in the presence of 2.5 mM AVS were analyzed by HPLC (Shimadzu, Tokyo, Japan) coupled to a UV detector (λ = 215 nm). An amount of 25 μL of the spent reaction of 5.0 mM glyoxal with 2.5 mM peroxynitrite in the presence of 2.5 mM AVS was injected into the HPLC equipment supplied with a Phenomenex Gemini C-18 column (250 mm × 4.6 mm i.d., particle size 5 μm). A gradient of methanol/acetonitrile (7:3, v:v) (solvent B) and 25 mM ammonium formate (solvent A) was used at a flow rate of 0.80 mL/min. The compounds were eluted by maintaining solvent B at 18% for 30 min and increasing solvent B from 18% to 65% over 5 min.

Identification of the AVS 9,10-endoperoxide generated by glyoxal/peroxynitrite was carried out in an HPLC system (Shimadzu, Tokyo, Japan) coupled to a Quattro II mass spectrometer (Micromass, Altricham, U.K). An amount of 20 μL of the spent reaction of 5.0 mM glyoxal with 2.5 mM peroxynitrite in the presence of 8.0 mM AVS was injected into the HPLC equipment supplied with a Phenomenex Luna C-18 column (250 mm × 4.6 mm i.d., particle size 5 μm). A gradient of methanol/acetonitrile (7:3, v:v) (solvent B) and 25 mM ammonium formate (solvent A) was used at a flow rate of 0.80 mL/min. The compounds were eluted by maintaining solvent B at 18% for 30 min, increasing solvent B from 18 to 80% over 10 min, and keeping solvent B at 80% for a further 5 min. Subsequently, solvent B was returned to the initial condition of 18% over 2 min and was kept at this concentration for 10 min. The negative multiple reactions monitoring (MRM) mode was used to monitor the specific mass transition of AVS $^{16}O_2$ (m/z 210−194) and AVS $^{18}O_2$ (m/z 212−194). The capillary voltage was set at 3.5 kV, collision energy at 10 eV, and the sample cone voltage and extractor cone voltage were at 10 and 4 V, respectively. The source and desolvation temperatures were maintained at 100 and 200 °C, respectively. The HPLC separation column and experimental conditions were the same as described above. The flow directed to the mass spectrometer was set at 0.20 mL/min.

Dioxygen labeling of AVS by $^{18}O_2$ was carried out by removing dissolved $^{16}O_2$ by successively freezing and thawing a solution of 8.0 mM AVS and 10.0 mM glyoxal in 1.0 mM D_3PO_4/D_2O under vacuum. This procedure was repeated at least three times to ensure complete removal of $^{16}O_2$. Thereafter, the whole system was connected to an $^{18}O_2$ gas cylinder at 0.5 atm and stirred for 5 min, followed by injection through a rubber seal of 100 μL of ice cold 45 mM peroxynitrite in D_2O prepared from the stock solution of peroxynitrite. Negative controls were run by replacing $^{18}O_2$ with pure $^{16}O_2$ or N_2.

Product Analysis by CE/UV. Analyses of formate were conducted in a Beckman P/551 capillary electrophoresis apparatus

dx.doi.org/10.1021/ja2051414 | J. Am. Chem.Soc. 2011, 133, 20761−20768

equipped with a filter-carousel UV detector set at 254 nm for indirect detection. The background electrolyte was 10 mM 3,5-dinitrobenzoic acid, with 0.10 mM cetyltrimethylammonium bromide and final pH equal to 3.2. Fused-silica capillaries with dimensions of 50 cm total length (40 cm effective) and 75 μm i.d. × 375 μm o.d. were used. Separation was performed at a constant voltage (−20 kV). Reaction mixture samples obtained from 1.0 to 10 mM glyoxal treated with 1.0−5.0 mM peroxynitrite were injected hydrodynamically at 1 psi for 3 s.

RESULTS AND DISCUSSION

Peroxynitrite Decay. Figure 1A shows time courses of peroxynitrite (200 μM) consumption by glyoxal (0−30 mM) monitored at 302 nm. The pseudo-first-order rate constants (k_{obs}) were found to increase linearly with the initial concentration of glyoxal, revealing an apparent second order rate constant ($k_{2,app}$) equal to 3.8×10^2 M^{-1} s^{-1} (Figure 1B). Because glyoxal dehydration in aqueous solution (pH 4−7) is a much slower process (about 10^{-2} M^{-1} s^{-1})[42] than the peroxynitrite carbonyl reaction and assuming that the glyoxal reactive carbonyl form is 0.005% of the nominal glyoxal concentration,[43] the k_2 value for the reaction can be estimated as 7.6×10^6 M^{-1} s^{-1}. This value is 3 orders of magnitude higher than that observed for the reaction with monocarbonyls, 2 orders of magnitude higher than that with diacetyl, and 1 order of magnitude higher than those reported with methylglyoxal and HCO_3^-/CO_2 at pH 7.2−7.4 and 25−37 °C ($(3-6) \times 10^4$ M^{-1} s^{-1}).[19,44,45] The glyoxal/peroxynitrite reaction is catalyzed by phosphate (Figure 1C), and the pH profile (Figure 1D) exhibits an ascendant curve from 6.2 to 7.2 with a trend for saturation above 7.2. This shape may reflect contributing effects of the pK_a values near 7.2 of both $H_2PO_4^-$ and peroxynitrous acid[21] at the phosphate ionic strength. Above 7.2, increasing concentration of peroxynitrite favors the reaction, while concomitant decrease of $H_2PO_4^-$ addition catalyst is counterbalanced by increased amounts of HPO_4^{2-}, which is expected to catalyze dehydration of glyoxal·H_2O to the carbonyl reactive form as reported by Thornalley et al.[43] for methylglyoxal.

Directed Flow EPR Studies. Classical spin-trapping studies with 2-methyl-2-nitrosopropane (MNP) aiming to intercept the MNP-formyl radical adduct failed, either because of a high instability of the radical itself or because of the radical adduct. Using continuous-flow EPR with direct detection, the peroxynitrite/glyoxal reaction was found to produce a triplet signal (1:2:1; a_H = 0.78 mT) in a glyoxal and peroxynitrite concentration-dependent fashion (parts A and B of Figure 2). The simulated spectrum is shown in Figure 2C. On replacement of glyoxal with formaldehyde, methanol, or ethanol under the same experimental conditions and equipment parameters, no signal was observed. This excludes possible interference of a carbon-centered radical bearing a hydrogen atom eventually formed from glyoxal products or contaminants. It is tempting to assign the 0.78 mT signal to the hydrated formyl radical, $^{\bullet}CH(OH)_2$ (half-life in aqueous medium of ~20 μs (reference), formed from β-cleavage of the oxyl radical, $CH(OH)_2-CH(OH)-O^{\bullet}$, which results from homolysis of the hypothetical peroxynitroso adduct of glyoxal, $CH(OH)_2-CH(OH)-OONO$. Because the putative $^{\bullet}CH(OH)_2$ radical is probably a poorer electrophile than the formyl radical toward MNP, accumulation of the MNP−$^{\bullet}CH(OH)_2$ adduct in the reaction mixture did not suffice to allow its EPR detection.

Interestingly, continuous-flow EPR experiments performed with peroxynitrite (200 μM)/glyoxal (30 mM) in the presence of MNP (20 mM) display a 1:2:2:1 quartet signal with $a_N = a_H$ = 1.44 mT, attributable to the MNP−H$^{\bullet}$ adduct[46−48] (Figure 3A). The triplet signal with a_N = 1.72 mT, also observed in the

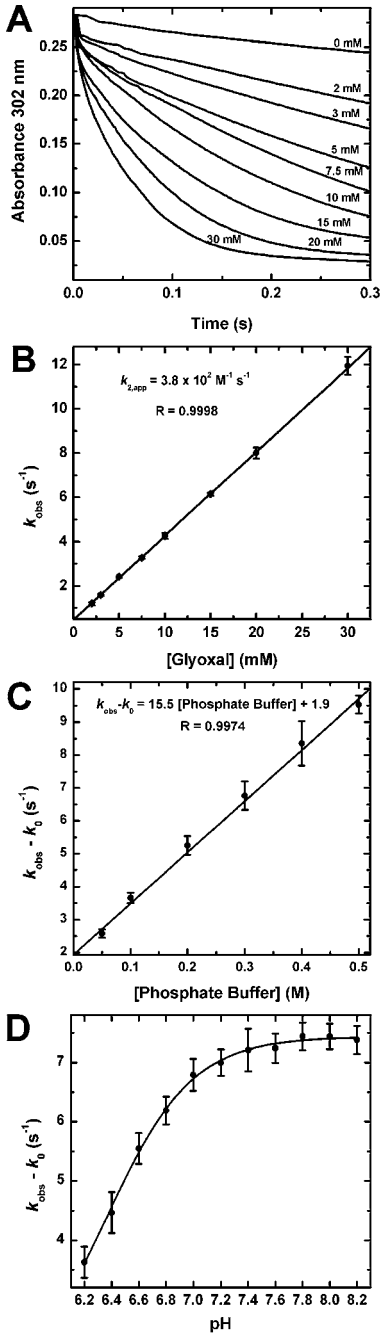

Figure 1. Stopped-flow kinetics of peroxynitrite decay in the presence of glyoxal. (A) Kinetic traces of peroxynitrite (200 μM) decay at different glyoxal concentrations (2.0−30 mM) in air equilibrated 250 mM phosphate buffer, pH 7.2, at 25 °C. (B) Pseudo-first-order rate constants (k_{obs}) for the decay of peroxynitrite in the presence of glyoxal under the same experimental conditions. Each k_{obs} value represents the mean of at least nine experiments. (C) Catalytic effect of phosphate anion on the observed rate of peroxynitrite (200 μM) treated with glyoxal (15 mM) at pH 7.2 and 25 °C. The ionic strength of the phosphate buffer was kept constant via the addition of NaCl. (D) pH profile of the reaction of glyoxal (15 mM) with peroxynitrite (200 μM) in air-equilibrated 350 mM phosphate buffer at 25 °C. The data represent the mean values of at least nine independent measurements.

dx.doi.org/10.1021/ja2051414 | J. Am. Chem.Soc. 2011, 133, 20761−20768

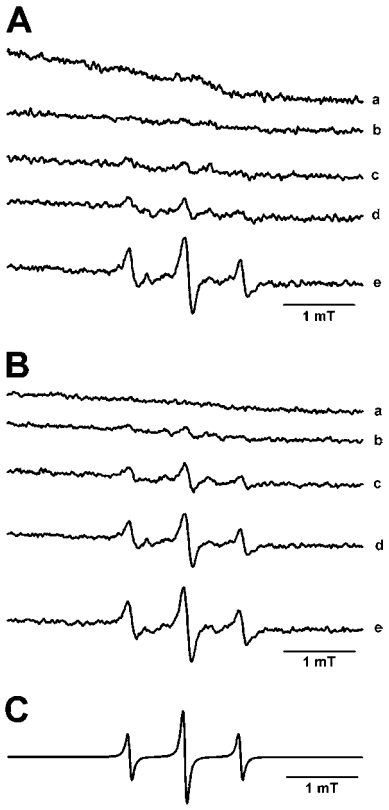

Figure 2. Direct EPR detection studies of the glyoxal/peroxynitrite system in 400 mM phosphate buffer, pH 7.2, at room temperature and a constant flow of 20 mL/min. (A) Spectra obtained from peroxynitrite (20 mM) without (a) and with (b) 220 mM, (c) 400 mM, (d) 500 mM, (e) 1.00 M glyoxal. (B) Spectra of glyoxal (1.0 M) without (a) and with (b) 5.0 mM, (c) 10 mM, (d) 20 mM, (e) 45 mM peroxynitrite. (C) Simulated spectrum obtained with a triplet signal 1:2:1 $a_{(0.5)}$ = 0.78 mT. Experimental conditions were as follows: observation time, 3.5 ms; microwave power, 10.13 mW; modulation amplitude, 0.1 mT; time constant, 163.84 ms; conversion time, 40.96 ms; gain, 1×10^6; two spectra accumulation.

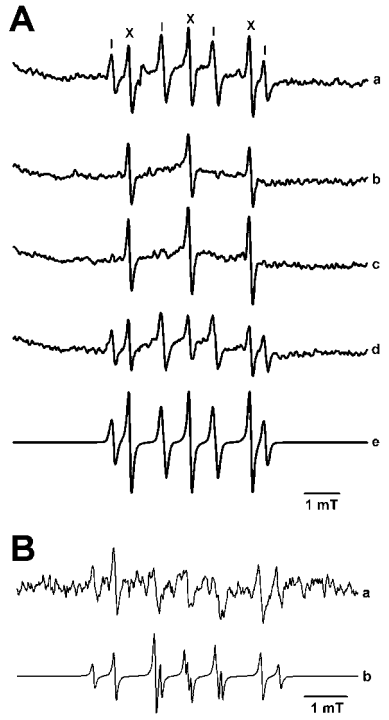

Figure 3. EPR continuous flow studies of the glyoxal/peroxynitrite system in the presence of MNP. An amount of 20 mM MNP was mixed with the glyoxal−peroxynitrite system in 200 mM phosphate buffer, pH 7.2, at room temperature and a constant flow of 1.4 mL/min. (A) Spectra obtained from (a) peroxynitrite (200 μM) plus glyoxal (30 mM), (b) peroxynitrite alone (200 μM), (c) glyoxal alone (30 mM), (d) peroxynitrite (200 μM) plus formaldehyde (30 mM), and (e) simulation composed from the signals a_N = 1.72 mT and a_N = a_H = 1.44 mT. (B) (a) EPR spectrum obtained from 750 μM peroxynitrite and 30 mM glyoxal, (b) simulated spectrum for the signals a_N = 1.72 mT, a_N = a_H = 1.44 mT and a_N = 0.71 mT and a_H = 0.14 mT. Experimental conditions for part A, traces a−d: observation time, 500 ms; microwave power, 10.11 mW; modulation amplitude, 0.1 mT; time constant, 163.84 ms; conversion time, 40.96 ms; gain, 1×10^6; accumulations, 8. Experimental conditions for part B, trace a: observation time, 500 ms; microwave power, 20.21 mW; modulation amplitude, 0.05 mT; time constant, 81.92 ms; conversion time, 40.96 ms; gain, 2×10^6; accumulations, 4.

control runs (200 μM peroxynitrite or 30 mM glyoxal in the spin trapping medium buffer), is due to the di-*tert*-butyl nitroxide signal (MNP contaminant)[49,50] (Figure 3A). Decarbonylation of the unstable formyl radical[51] is indeed expected to release a hydrogen atom that can reduce MNP. Accordingly, photolysis and one-electron oxidation of formaldehyde by oxidants in the gas phase, including HO$^\bullet$ radical, are long known to form CO and H_2 probably via a formyl radical intermediate.[52] In aerated aqueous solutions, oxidation of formaldehyde by H_2O_2-generated HO$^\bullet$ radical during laser photolysis experiments was found to yield formic acid and CO, which also implies the intermediacy of $^\bullet CH(OH)_2$ radical.[53] Furthermore, glyoxal photoexcited at 395−414 nm in the gas phase has recently been reported as a chemical source of formyl radical, which decomposes to CO and H_2.[54] In the current experiments, replacement of glyoxal with formaldehyde (30 mM) produced the same MNP spin adduct that was formed with glyoxal (quartet, a_N = a_H = 1.44 mT) (Figure 3A), supporting the hypothesis of MNP reduction by hydrogen atom.

The bottom spectrum in Figure 3A is the simulation of the mixture of radicals from glyoxal/peroxynitrite reaction and MNP contaminants. However, a reaction mixture containing 750 μM peroxynitrite and 30 mM glyoxal in the presence of 20 mM MNP (Figure 3B, trace a) exhibits an additional signal, which is attributable to the MNP−formyl radical adduct (a_N = 0.71 mT; a_H = 0.14 mT; lit. data a_N = 0.69−0.77 mT and a_H = 0.14−0.25 mT).[46,55,56] The bottom trace in Figure 3B depicts the simulated spectrum obtained from the signals attributable to MNP contaminant (a_N = 1.72 mT), the MNP-H$^\bullet$ radical adduct (a_N = a_H = 1.44 mT), and the MNP−formyl radical adduct (a_N = 0.69−0.77 mT; a_H = 0.14−0.25 mT).

Monomolecular Photoemission of Singlet Oxygen at 1270 nm. The well-known monomol emission of O_2 ($^1\Delta_g$) at 1270 nm[57] was observed from the peroxynitrite/glyoxal reaction conducted in normally aerated phosphate buffer in D_2O. The chemiluminescence intensity increases upon raising the concentration of peroxynitrite (Figure 4A) and of glyoxal to 25 mM (Figure 4B). Upon addition of singlet oxygen quenchers such as L-histidine and NaN_3 or by replacement of D_2O with H_2O-buffered solution,[58,59] the red emission intensity was not observed (Figure 4C). That a putative formylperoxyl radical intermediate is the source of O_2 ($^1\Delta_g$) is endorsed by the lack of enhanced infrared emission when

dx.doi.org/10.1021/ja2051414 | J. Am. Chem.Soc. 2011, 133, 20761−20768

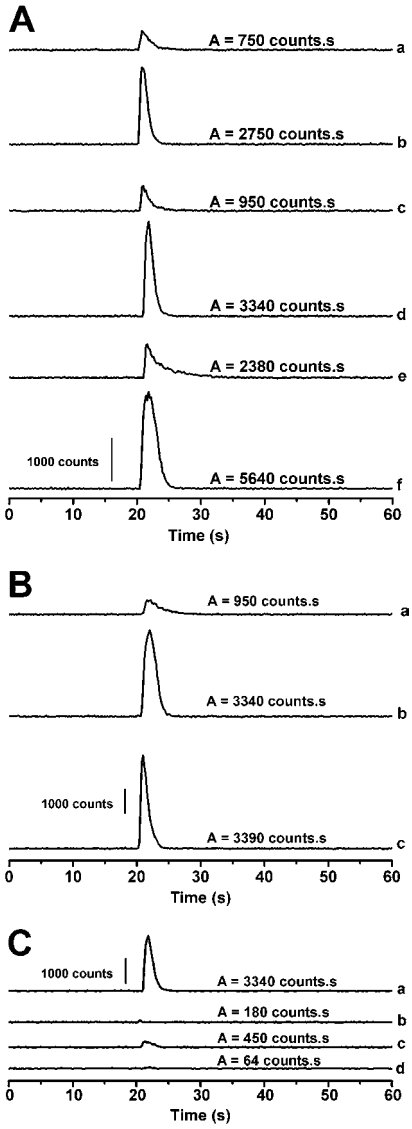

Figure 4. Monomol emission of singlet ($^1\Delta_g$) molecular oxygen observed from the glyoxal–peroxynitrite system. Normally aerated 250 mM phosphate buffer prepared in D_2O, pD 7.2, contained (A) 1.0 mM peroxynitrite without (a) and with 5.0 mM glyoxal (b), 2.5 mM peroxynitrite without (c) and with 5.0 mM glyoxal (d), 5.0 mM peroxynitrite without (e) and with 5.0 mM glyoxal (f). (B) Peroxynitrite without (a) and with 5.0 mM (b) or 25 mM (c) glyoxal. (C) 2.5 mM peroxynitrite and 5.0 mM glyoxal without (a) and in the presence of H_2O, pH 7.2 (b), 2.5 mM L-histidine (c), and 2.5 mM NaN_3 (d).

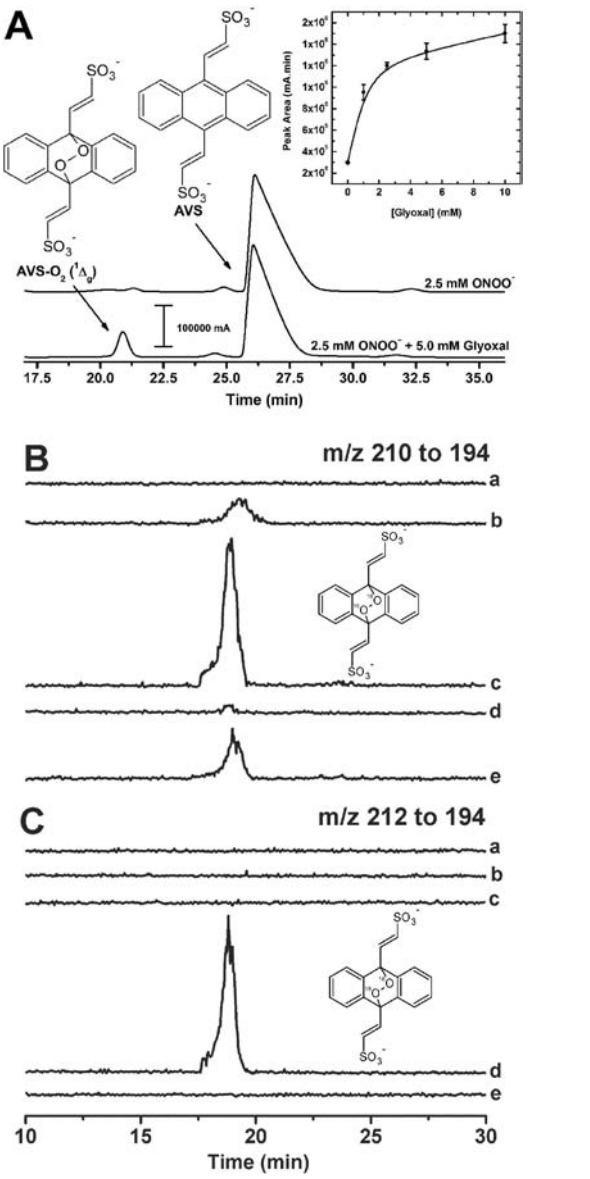

Figure 5. Chemical trapping studies of singlet ($^1\Delta_g$) $^{16}O_2$ and $^{18}O_2$ with AVS. (A) HPLC/UV traces for chemical-trapping of O_2 ($^1\Delta_g$). Reaction mixture was 5.0 mM glyoxal, 2.5 mM peroxynitrite, and 2.5 mM AVS in normally aerated 500 mM D_2O buffer, pD 7.2. Inset: Concentration effect of glyoxal (1.0–10 mM) on the peak area attributed to the AVS reaction product with O_2 ($^1\Delta_g$). (B) HPLC/MS/MS evidence for the specific transition of AVS $^{16}O_2$ to AVS (m/z 210–194) in the MRM mode. Complete reaction mixture was 10.0 mM glyoxal, 2.0 mM peroxynitrite, and 8.0 mM AVS in 1.0 mM D_3PO_4/D_2O, final pD in the range 6.8–7.4. (a) glyoxal + AVS under $^{16}O_2$; (b) peroxynitrite + AVS under $^{16}O_2$; (c) peroxynitrite + glyoxal + AVS under $^{16}O_2$; (d) peroxynitrite + glyoxal + AVS under $^{18}O_2$; (e) peroxynitrite + glyoxal + AVS under N_2. (C) Same as (B) by monitoring the specific transition of AVS $^{18}O_2$ to AVS (m/z 212–194) in the MRM mode.

glyoxal is replaced by diacetyl or methylglyoxal under identical experimental conditions (not shown). Upon reaction with peroxynitrite these reagents yield acetyl radicals that do not display a geminal hydrogen necessary to ultimately undergo the Russell reaction.

Chemical Trapping of Singlet Oxygen and HPLC/UV and HPLC/MS Analysis. Another specific and sensitive approach commonly used to detect O_2 ($^1\Delta_g$) is chemical trapping coupled to HPLC/MS/MS. In this experiment, we used AVS, a chemical trap that is known to react with O_2 ($^1\Delta_g$), yielding the corresponding 9,10-endoperoxide ($AVSO_2$). The yield of $AVSO_2$, determined by HPLC/UV at 215 nm, was found to be dependent on glyoxal concentration (1.0–10 mM) (Figure 5A). Formation of O_2 ($^1\Delta_g$) in the reaction was also evaluated by HPLC/MS/MS in the MRM mode, monitoring the specific conversion of $AVSO_2$ to AVS (m/z 210–194) (Figure 5B, trace c). The intense peak at 18 min was identified in the MRM chromatogram as $AVSO_2$, since it displays the same retention time and fragmentation pattern as an $AVSO_2$ standard generated by photooxidation (data not shown).[38] One can estimate that the reaction studied here generates ~2% of

dx.doi.org/10.1021/ja2051414 | J. Am. Chem.Soc. 2011, 133, 20761–20768

molecular oxygen in the $^1\Delta_g$ state considering the nominal peroxynitrite concentration (from the observed consumption of AVS (8.0 mM), evaluated by the corresponding HPLC/UV peak area when in the presence of the glyoxal (10.0 mM)/peroxynitrite (2.0 mM) system) and considering that (i) one molecule of O_2 ($^1\Delta_g$) requires two formylperoxyl radicals, (ii) the Russell reaction forms ~10% O_2 ($^1\Delta_g$),[28] and (iii) the chemical yield of O_2 ($^1\Delta_g$) trapping by AVS is about 50%. As expected from work published elsewhere,[60] peroxynitrite alone gives rise to O_2 ($^1\Delta_g$) at lower yields, as shown in traces b and e of Figure 5B. That the oxygen atoms of $AVSO_2$ are not derived exclusively from peroxynitrite was confirmed by repeating the experiment under N_2 (Figure 5B, trace e) compared to normally aerated solution (Figure 5B, trace c).

Unequivocal evidence for glyoxal/peroxynitrite-generated O_2 ($^1\Delta_g$) cycloadition to AVS by a mechanism involving a Russell reaction of formylperoxyl radical intermediate was provided by oxygen labeling experiments with $^{18}O_2$. The MRM trace of the 212−194 transition depicted by Figure 5C, trace d, shows that in $^{18}O_2$-purged solutions, treatment of glyoxal with peroxynitrite renders almost exclusively AVS $^{18}O_2$. Control experiments described in the caption to the figure show no AVS $^{18}O_2$ formation. Furthermore, generation of small amounts of AVS $^{16}O_2$ in the experiment performed with $^{18}O_2$-purged solutions (Figure 5B, trace d) may be due to peroxynitrite[60] and/or a dioxirane intermediate[16] acting as a minor source of O_2 ($^1\Delta_g$).

Formate Analysis. Formate was the main product detected by CE-UV in the final reaction mixture from the glyoxal/peroxynitrite system (Figure 6). Consistent with the

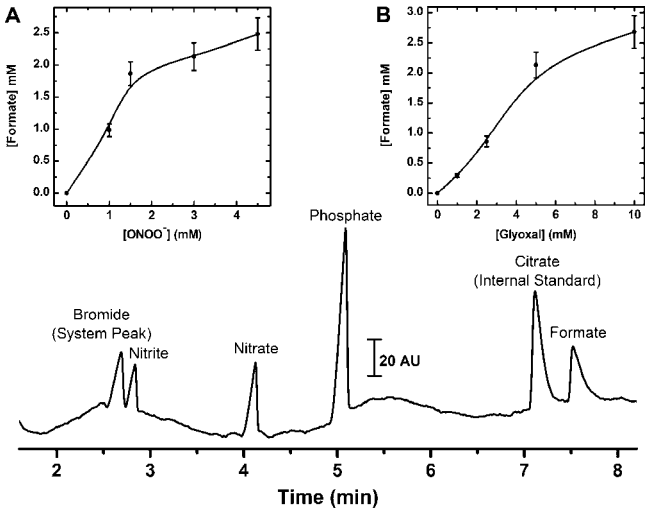

Figure 6. CE-UV electropherogram obtained for the final reaction mixture of glyoxal (2.5 mM) treated with peroxynitrite (1.5 mM). Citrate (1 mM) was added as an internal standard. Inset: Dependence of formate ion yield on the concentrations of peroxynitrite and glyoxal. (A) Peroxynitrite (1.0−4.5 mM) in the presence of 5.0 mM glyoxal. (B) Peroxynitrite (3.0 mM) in the presence of glyoxal (1.0−10 mM).

hypothetical intermediacy of a nitrosoperoxy carbonyl adduct, whose homolysis yields $^{\bullet}NO_2$,[17,18] an increased nitrite/nitrate ratio is expected to be found in the spent reaction mixture.[16,17] However, the concentration of these anions is normally high in peroxynitrite stock solutions, thereby offering low analytical accuracy and allowing detection of just a trend for relative increase of nitrite. The equipment was calibrated with a mixture of nitrite, nitrate, phosphate, glyoxalate, formate, and oxalate at known concentrations, and citrate was used as an internal standard. The insets in Figure 6 show the dependence of formate concentration in the final reaction mixture on reacting glyoxal (1.0−10 mM) and peroxynitrite (1.0−5.0 mM) under continuous vortex aeration. Using 1.5 mM peroxynitrite and 4.5 mM glyoxal (inset B), 2.0 mM formate was found from curve deflection. Assuming peroxynitrite reacts stoichiometrically with glyoxal and each glyoxal molecule can generate maximally two formate ions, the chemical yield of formate is roughly 66%.

The absence of glyoxalate and oxalate in the final reaction mixtures indicates that partial oxidation of glyoxal by peroxynitrite does not occur. These results attest that the reaction proceeds by an initial step of nucleophilic addition of peroxynitrite to glyoxal, followed by oxidative fragmentation to formate ion in the presence of molecular oxygen, as previously reported for other peroxynitrite-treated α-dicarbonyls.[14,15]

Potential Biological Implications. Singlet oxygen is a strong electrophile known to react with various biomolecules, including nucleic acids, proteins, and lipids. It has been suggested to play beneficial and deleterious cellular roles including in cell signaling cascades associated with apoptosis and in genetically controlled death of plants. To date, singlet oxygen is reportedly formed in vivo (i) chemically, from ClO^- anion and peroxides (e.g., H_2O_2, $ONOO^-$) and from dismutation of $ROO^{\bullet}$ radicals derived from polyunsaturated fatty acids, nucleobases, and amino acids, (ii) enzymatically from prostaglandin cyclooxygenase, hemoglobin or myoglobin/H_2O_2, and lactoperoxidase/H_2O_2, (iii) UVA radiation, or (iv) through photosensitization of molecular oxygen by endogenous (e.g., protoporphyrin IX) and xenobiotic dyes used in photodynamic therapy.[57−64]

Although normally present at very low concentrations in tissues, glyoxal and peroxynitrite are accumulated in some human disorders and might spark adverse responses associated with the chemistry of singlet ($^1\Delta_g$) molecular oxygen. For example, glyoxal concentration is reportedly in the range 0.05−0.08 μg/mL in serum[65] and 12.5 ± 0.5 μg/L in plasma[66] of healthy individuals but reaches 0.19−0.33 μg/mL [65] in serum, 22.6 ± 3 μg/mL in plasma,[66] and 0.18−0.40 μg/mL [65] in the urine of diabetes patients. On the other hand, very high fluxes (>2 μM/s) of $NO^{\bullet}/O_2^{\bullet-}$ were found to be required in vitro to yield peroxynitrite at concentrations able to ultimately accomplish tyrosine nitration and dimerization.[67] Nevertheless, the relevance of the glyoxal/peroxynitrite pair in biological systems must be considered in light of the complex spatiality and temporality of cellular events.[68] These are governed by cell compartmentalization, metabolism, and duration of toxicant exposure, in addition to concentration factors, intermediate lifetimes, and reaction rate constants. Thus, it is tempting to propose that the glyoxal−peroxynitrite reaction may take place chronically in tissue microenvironments under adverse oxidative, nitrosative, and carbonyl stress, as is the case of inflammation sites.

Noteworthy, on the basis of the short lifetime and lack of chemical selectivity of such highly oxidant species, a role of singlet ($^1\Delta_g$) molecular oxygen as well as of hydroxyl radical in cell signaling was recently questioned by Forman et al.[68] However, secondary products of singlet oxygen activity may influence cell signaling. For example, a cholesterol carboxaldeyde specifically formed from cholesterol oxidation by singlet oxygen or exogenous ozone,[69] and implicated in the pathophysiology of atherosclerosis and Alzheimer diseases, induces cytotoxicity in cardiomyocytes through an H_2O_2 and

dx.doi.org/10.1021/ja2051414 | J. Am. Chem.Soc. 2011, 133, 20761−20768

p38 mitogen activated protein kinase-mediated signaling process.[70]

CONCLUSION

The reaction of glyoxal with peroxynitrite in aerated medium is envisaged here as being initiated by phosphate-catalyzed peroxynitrite addition to glyoxal to form a hypothetical nitrosoperoxy intermediate (Scheme 1). Subsequent homolysis

Scheme 1. Chemical Mechanism Proposed for the Generation of Singlet Oxygen from the Glyoxal–Peroxynitrite System in Aerated Phosphate Buffer, pH 7.2

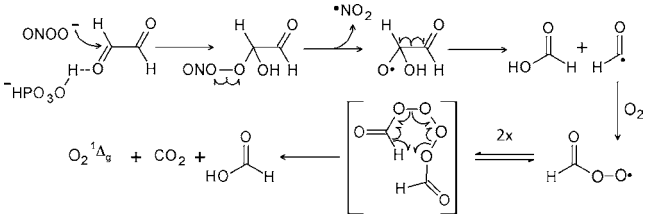

of this intermediate yields $^{\bullet}NO_2$ and a glyoxal-derived oxyl radical. β-Cleavage of the latter radical is expected to generate formate ion and formyl radical, followed by formyl radical annihilation by molecular oxygen to a formylperoxyl radical. By virtue of displaying a geminal hydrogen, the formylperoxyl radical is prone to dismutation (Russell reaction) yielding molecular oxygen in the singlet ($^1\Delta_g$) state, formic acid, and CO_2. This mechanism is strongly supported by (i) the observed concentration-dependent phosphate-catalyzed peroxynitrite consumption by glyoxal (Figure 1), ultimately yielding formate as the only product (Figure 6), (ii) direct flow EPR experiments with glyoxal/peroxyntrite in the presence of MNP which reveal a radical adduct with hydrogen atom expectedly formed from formyl radical decarbonylation (Figures 2 and 3), and (iii) detection of the monomolecular emission of singlet oxygen ($^1\Delta_g$) at 1270 nm in buffered D_2O, which can be quenched by L-histidine and azide ion and trapped with AVS to form the corresponding 9,10-endoperoxide.

AUTHOR INFORMATION

Corresponding Author

ejhbechara@gmail.com

ACKNOWLEDGMENTS

We are grateful to Dr. B. Bandy (University of Saskatchewan, Canada) for kindly reading the manuscript and F. M. Prado for technical assistance. Funding sources for this work are the following: Fundação de Amparo à Pesquisa do Estado de São Paulo (FAPESP), the Conselho Nacional de Desenvolvimento Científico e Tecnológico (CNPq), and the Instituto Nacional de Ciência e Tecnologia (INCT) de Processos Redox em Biomedicina (Redoxoma).

DEDICATION

‖Dedicated to Dr. Thérése Wilson (Harvard University, MA).

REFERENCES

(1) Gobert, J.; Glomb, M. A. *J. Agric. Food Chem.* **2009**, *57*, 8591.
(2) Kuntz, S.; Rudloff, S.; Ehl, J.; Bretzel, R. G.; Kunz, C. *Eur. J. Nutr.* **2009**, *48*, 499.
(3) Darowska, A.; Borcz, A.; Nawrocki. *J. Food Addit. Contam.* **2003**, *20*, 1170.
(4) da Silva Ferreira, A. C.; Reis, S.; Rodrigues, C.; Oliveira, C.; de Pinho, P. G. *J. Food Sci.* **2007**, *72*, S314.
(5) Neng, N. R.; Cordeiro, C. A.; Freire, A. P.; Nogueira, J. M. *J. Chromatogr., A* **2007**, *1169*, 47.
(6) Fujioka, K.; Shibamoto, T. *Environ. Toxicol.* **2006**, *21*, 47.
(7) Liu, W.; Zhang, J.; Know, J.; Weisel, C.; Turping, B.; Zhang, L.; Korn, L.; Morandi, M.; Stock, T.; Colome, S. *J. Air Waste Manage. Assoc.* **2006**, *56*, 1196.
(8) Salter, R. J.; Blitz, M. A.; Heard, D. E.; Pilling, M. J.; Seakins, P. W. *J. Phys. Chem. A* **2009**, *113*, 8278.
(9) Ho, S. S.; Yu, J. Z.; Chu, K. W.; Yeung, L. L. *J. Air Waste Manage. Assoc.* **2006**, *56*, 1091.
(10) Grillo, M. A.; Colombatto, S. *Amino Acids* **2008**, *35*, 29.
(11) Murata-Kamiya, N.; Kamiya, H.; Iwamoto, N.; Kasai, H. *Carcinogenesis* **1995**, *16*, 2251.
(12) Awada, M.; Dedon, P. C. *Chem. Res. Toxicol.* **2001**, *14*, 1247.
(13) Thornalley, P. J. *Drug Metab. Drug Interact.* **2008**, *23*, 125.
(14) Massari, J.; Tokikawa, R.; Zanolli, L.; Tavares, M. F. M.; Assunção, N. A.; Bechara, E. J. H. *Chem. Res. Toxicol.* **2010**, *23*, 1762.
(15) Massari, J.; Fujiy, D. E.; Dutra, F.; Vaz, S. M.; Costa, A. C. O.; Micke, G. A.; Tavares, M. F. M.; Tokikawa, R.; Assunção, N. A.; Bechara, E. J. H. *Chem. Res. Toxicol.* **2008**, *21*, 879.
(16) Yang, D.; Tang, T.; Chen, J.; Wang, X.; Bartberger, M. D.; Houk, K. N.; Olson, L. *J. Am. Chem. Soc.* **1999**, *121*, 11976.
(17) Uppu, R. M.; Winston, G. W.; Pryor, W. A. *Chem. Res. Toxicol.* **1997**, *10*, 1331.
(18) Nakao, L. S.; Ouchi, D.; Augusto, O. *Chem. Res. Toxicol.* **1997**, *12*, 1010.
(19) Medinas, D. B.; Cerchiaro, G.; Trindade, D. F.; Augusto, O. *IUBMB Life* **2007**, *59*, 255.
(20) Augusto, O.; Bonini, M. G.; Amanso, A. M.; Linares, E.; Santos, C. C.; Menezes, S. L. *Free Radical Biol. Med.* **2002**, *32*, 841.
(21) Lobachev, V. L.; Rudakov, E. S. *Russ. Chem. Rev.* **2006**, *75*, 375.
(22) Ferrer-Sueta, G.; Radi, R. *ACS Chem. Biol.* **2009**, *4*, 161.
(23) Pacher, P.; Beckman, J. S.; Liaudet, L. *Physiol. Rev.* **2007**, *87*, 315.
(24) Szabó, C.; Ischiropoulos, H.; Radi, R. *Nat. Rev. Drug Discovery* **2007**, *6*, 662.
(25) Radi, R. *Proc. Natl. Acad. Sci. U.S.A.* **2004**, *101*, 4003.
(26) Goldstein, S.; Merényi, G. *Methods Enzymol.* **2008**, *436*, 49.
(27) Rebrin, I.; Bregere, C.; Gallaher, T. K.; Sohal, R. S. *Methods Enzymol.* **2008**, *441*, 283.
(28) Niu, Q.; Mendenhall, G. D. *J. Am. Chem. Soc.* **1992**, *114*, 165.
(29) Russell, G. A. *J. Am. Chem. Soc.* **1957**, *79*, 3871.
(30) Russell, G. A. *J. Am. Chem. Soc.* **1955**, *77*, 4583.
(31) Russell, G. A. *J. Am. Chem. Soc.* **1956**, *78*, 1047.
(32) Howard, J. A.; Ingold, K. U. *J. Am. Chem. Soc.* **1968**, *90*, 1056.
(33) Kanofsky, J. R.; Axelrod, B. *J. Biol. Chem.* **1986**, *261*, 1099.
(34) Beckman, J. S.; Beckman, T. W.; Chen, J.; Marshall, P. A.; Freeman, B. A. *Proc. Natl. Acad. Sci. U. S. A.* **1990**, *87*, 1620.
(35) Beers, R. F.; Sizer, W. I. *J. Biol. Chem.* **1952**, *195*, 133.
(36) Hughes, M. N.; Nicklin, H. G. *J. Chem. Soc. A* **1968**, 450.
(37) Nardello, V.; Aubry, J. I. M.; Johnston, P.; Bulduk, I.; de Vries, A. H. M.; Alsters, P. L. *Synlett* **2005**, 2667.
(38) Prado, F. M.; Oliveira, M. C. B.; Miyamoto, S.; Martinez, G. R.; Medeiros, M. H. G.; Ronsein, G. E.; Di Mascio, P. *Free Radical Biol. Med.* **2009**, *47*, 401.
(39) Duling, D. R. *J. Magn. Reson.* **1994**, *104*, 105.
(40) Miyamoto, S.; Martinez, G. R.; Medeiros, M. H. G.; Di Mascio, P. *J. Am. Chem. Soc.* **2003**, *125*, 6172.
(41) Miyamoto, S.; Martinez, G. R.; Martins, A. P. B; Medeiros, M. H. G.; Di Mascio, P. *J. Am. Chem. Soc.* **2003**, *125*, 4510.
(42) Betterton, E. A.; Hoffmann, M. R. *J. Phys. Chem.* **1987**, *91*, 3011.
(43) Thornalley, P. J.; Yurek-George, A.; Argirov, O. K. *Biochem. Pharmacol.* **2000**, *60*, 55.
(44) Denicola, A.; Freeman, B. A.; Trujillo, M.; Radi, R. *Arch. Biochem. Biophys.* **1996**, *333*, 49.

(45) Lymar, S. V.; Hurst, J. K. *J. Am. Chem. Soc.* **1995**, *117*, 8867.
(46) Buettner, G. R. *Free Radical Biol. Med.* **1987**, *3*, 259.
(47) Kennedy, C. H.; Pryor, W. A.; Winston, G. W.; Church, D. F. *Biochem. Biophys. Res. Commun.* **1986**, *141*, 1123.
(48) Chignell, C. F.; Kalyanaraman, B.; Mason, R. P.; Sik, R. H. *Photochem. Photobiol.* **1980**, *32*, 563.
(49) Gunther, M. R.; Peters, J. A.; Silvaneri, M. K. *J. Biol. Chem.* **2002**, *277*, 9160.
(50) Makino, K.; Suzuki, N.; Moriya, F.; Rokushika, S.; Hatano, H. *Radiat. Res.* **1981**, *86*, 294.
(51) Troe, J. *J. Phys. Chem. A* **2007**, *111*, 3868.
(52) Carbajo, P. G.; Smith, S. C.; Holloway, A.-L.; Smith, C. A.; Pope, F. D.; Shallcross, D. E.; Orr-Ewing, A. J. *J. Phys. Chem. A* **2008**, *112*, 12437.
(53) McElroy, W. J.; Waygood, S. J. *J. Chem. Soc., Faraday Trans.* **1991**, *87*, 1513.
(54) Salter, R. J.; Blitz, M. A.; Heard, D. E.; Pilling, M. J.; Seakins, P. W. *J. Phys. Chem. A* **2009**, *113*, 8278.
(55) Janzen, E. G.; Lopp, I. G.; Morgan, T. V. *J. Phys. Chem.* **1973**, *77*, 139.
(56) Heinzel, A.; Holze, R.; Hamann, C. H.; Blum, J. K. *Electrochim. Acta* **1989**, *34*, 657.
(57) Khan, A. U.; Kasha, M. *J. Am. Chem. Soc.* **1970**, *92*, 3293.
(58) Lengfelder, E.; Cadenas, E.; Sies, H. *FEBS Lett.* **1983**, *164*, 366.
(59) Krinsky, N. I. *Trends Biochem. Sci.* **1977**, *2*, 35.
(60) Miyamoto, S.; Ronsein, G. E.; Corrêa, T. C.; Martinez, G. R.; Medeiros, M. H. G.; Di Mascio, P. *Dalton Trans.* **2009**, 5720.
(61) Miyamoto, S.; Ronsein, G. E.; Prado, F. M.; Uemi, M.; Corrêa, T. C.; Toma, I. N.; Bertolucci, A.; Oliveira, M. C. B.; Motta, F. D.; Medeiros, M. H. G.; Di Mascio, P. *IUBMB Life* **2007**, *59*, 322.
(62) Schweitzer, C.; Schmidt, R. *Chem. Rev.* **2003**, *103*, 1685.
(63) Cadet, J.; Douki, T.; Ravanat, J.-L.; Di Mascio, P. *Photochem. Photobiol. Sci.* **2009**, *8*, 903.
(64) Alarcón, E.; Henríquez, C.; Aspée, A.; Lissi, E. A. *Photochem. Photobiol.* **2007**, *83*, 475.
(65) Zardari, L. A.; Khuhawar, A. J.; Laghari, A. J. *Chromatographia* **2009**, *70*, 891.
(66) Lapolla, A.; Flamini, R.; Lupo, A.; Aricò, N. C.; Rugiu, C.; Reitano, R.; Tubaro, M.; Regazzi, E.; Seraglia, R.; Traldi, P. *Ann. N.Y. Acad. Sci.* **2005**, *1043*, 217.
(67) Pfeiffer, S.; Schmidt, K.; Mayer, B. *J. Biol. Chem.* **2000**, *275*, 6346.
(68) Forman, H. J.; Maiorino, M.; Ursini, F. *Biochemistry* **2010**, *49*, 835.
(69) Uemi, M.; Ronsein, G. E.; Miyamoto, S.; Medeiros, M. H. G.; Di Mascio, P. *Chem. Res. Toxicol.* **2009**, *22*, 875.
(70) Laynes, L.; Raghavamenon, A. C.; D'Auvergne, O.; Achuthan, V.; Uppu, R. M. *Biochem. Biophys. Res. Commun.* **2011**, *404*, 90.